

ATTENTION HEAD PURIFICATION: A NEW PERSPECTIVE TO HARNESS CLIP FOR DOMAIN GENERALIZATION

Anonymous authors

Paper under double-blind review

ABSTRACT

Domain Generalization (DG) aims to learn a model from multiple source domains to achieve satisfactory performance on unseen target domains. Recent works introduce CLIP to DG tasks due to its superior image-text alignment and zero-shot performance. Previous methods either utilize full fine-tuning or prompt-learning paradigms to harness CLIP for DG tasks. Those works focus on avoiding catastrophic forgetting of the original knowledge encoded in CLIP but ignore that the knowledge encoded in CLIP in nature may contain domain-specific cues that constrain its domain generalization performance. In this paper, we propose a new perspective to harness CLIP for DG, *i.e.*, attention head purification. We observe that different attention heads may encode different properties of an image and selecting heads appropriately may yield remarkable performance improvement across domains. Based on such observations, we purify the attention heads of CLIP from two levels, including *task-level purification* and *domain-level purification*. For task-level purification, we design head-aware LoRA to make each head more adapted to the task we considered. For domain-level purification, we perform head selection via a simple gating strategy. We utilize MMD loss to encourage masked head features to be more domain-invariant to emphasize more generalizable properties/heads. During training, we jointly perform task-level purification and domain-level purification. We conduct experiments on various representative DG benchmarks. Though simple, extensive experiments demonstrate that our method performs favorably against previous state-of-the-arts.

1 INTRODUCTION

Deep learning has attained remarkable success on various downstream tasks in computer vision, typically under the assumption that both training and test samples are identically distributed. However, in practice, test data distributions (target) are usually different from the training ones (source). In such cases, the performance of deep neural networks may degenerate severely on target, showing a poor domain generalization ability. To mitigate the domain shift, a series of Domain Generalization (DG) methods (Carlucci et al., 2019; Cha et al., 2022; Gulrajani & Lopez-Paz, 2020; Kim et al., 2022; Li et al., 2018a;b; Zhou et al., 2021) are proposed to transfer the knowledge learned from multiple source domains to unseen target domains, via domain-invariant learning (Wang et al., 2022; Jia et al., 2020; Li et al., 2020; 2018c; Shao et al., 2019; Wang et al., 2021), meta-learning techniques (Sankaranarayanan & Balaji, 2023; Balaji et al., 2018b;a; Li et al., 2018a), or specifically-designed data augmentations (Volpi et al., 2018; Qiao et al., 2020; Zhou et al., 2020a). The remarkable progress achieved by those works can be largely attributed to a well-initialized feature extractor provided by ImageNet-pretrained (Huh et al., 2016) backbones. Recent proposed Contrastive Language–Image Pre-training (*i.e.*, CLIP (Radford et al., 2021)) learns from large amounts of image-text pairs (Jia et al., 2021) and demonstrates impressive zero-shot learning performance. It may potentially serve as a better foundation for mitigating the performance gap across domains for specific downstream tasks.

Despite superior zero-shot classification performance of CLIP, it is not trivial to harness CLIP for specific domain generalization tasks beyond its zero-shot classification ability. Directly fine-tuning CLIP may obtain even worse performance than zero-shot classification (Pham et al., 2023; Wortsman et al., 2022). Previous works tackle this issue mainly by introducing various regularizations to avoid

054
055
056
057
058
059
060
061
062
063
064
065
066
067
068
069
070
071
072
073
074
075
076
077
078
079
080
081
082
083
084
085
086
087
088
089
090
091
092
093
094
095
096
097
098
099
100
101
102
103
104
105
106
107

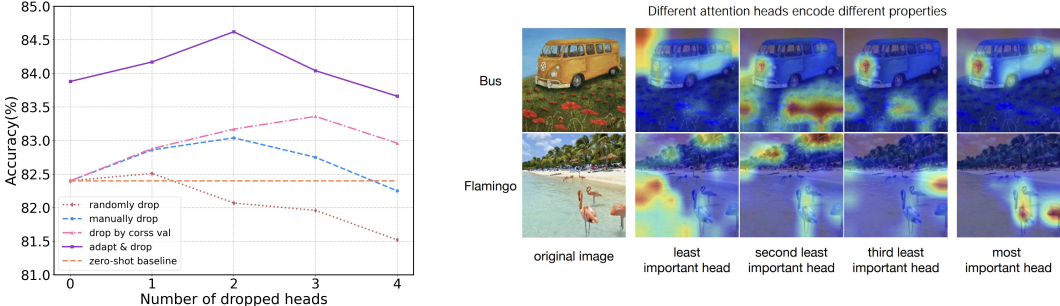


Figure 1: **Left:** We use different strategies to evaluate the importance of each attention head on domain generalization and drop the least important ones to see how accuracy changes. The strategies we adopt include “randomly drop(−◇−)”, “manually drop(−●−)”, “drop by cross-validation(−▲−)”, and “adapt & drop(−■−)”. Details of strategies can be found in Appendix. Via appropriately dropping heads, CLIP’s domain generalization performance can be improved. **Right:** Attention map (Chefer et al., 2021) generated by specific heads. The middle columns are from least important heads determined by the cross-validation strategy. They all capture lots of background information. The last column represents the most important one whose attention map mainly focuses on the object itself. The experiments are conducted on OfficeHome (Venkateswara et al., 2017). Best viewed in color.

the forgetting of original knowledge encoded in CLIP. For example, Shu et al. (2023) fully fine-tunes CLIP’s image encoder with modified contrastive loss to mitigate overfitting and proposes beta moving average to perform a temporal ensembling along the fine-tuning trajectory. Cha et al. (2022) proposes mutual information regularization between the original CLIP and the fine-tuned one to prevent the two models from deviating too much. Although those works achieve improved domain generalization performance, a natural question arises: *is the way to avoid knowledge forgetting sufficient to harness CLIP for domain generalization?*

Recent work (Gandelsman et al., 2023) shows that different attention heads of CLIP’s image encoder (ViT-based) may encode different properties of an image. Inspired by this work, we conduct ablation experiments to verify the effectiveness of each head in the context of domain generalization. Specifically, we utilize different ways to evaluate the importance of attention heads on domain generalization (e.g., manual evaluation, evaluation by cross-validation, etc.) and drop the least important ones. As shown in Figure 1(a), we observe that via appropriately dropping some attention heads, we may achieve a much better domain generalization performance. **This phenomenon implies that not all attention heads are domain generalizable and some heads may harm the domain generalization ability of CLIP, which means those heads may contain non-generalizable cues (i.e., domain-specific cues).** To further illustrate our findings, we provide attention visualizations in Figure 1(b). We observe that the attention maps (Chefer et al., 2021) of the least important heads mainly highlight task-irrelevant regions like background, while the most important head pays more attention to the object itself. As a result, simply avoiding the knowledge forgetting of CLIP may not be optimal for domain generalization tasks. We need to purify the attention heads to make CLIP more task-adapted and domain-generalizable.

In this paper, we propose a new perspective to harness CLIP for domain generalization tasks, i.e., through attention head purification. Specifically, we perform two kinds of attention head purification during training, which are named *task-level purification* and *domain-level purification*. For task-level purification, we aim to purify the attention head of CLIP to maintain more task-related knowledge. Technically, we adopt LoRA to realize this goal. Different from conventional LoRA implementation, we design head-aware LoRA (HA-LoRA) to purify and adapt each head more accordingly. For domain-level purification, we aim to purify the attention heads of CLIP to make the resulting features more invariant across domains. We design a simple learnable gating strategy to select the heads that most benefit the domain generalization performance. To realize this, in addition to the cross-entropy loss on source images, we utilize Maximize Mean Discrepancy (MMD) loss to encourage the gates to emphasize more domain-invariant head features. Note that we do not utilize the gradients of MMD loss to update the HA-LoRA. In this way, we may decouple task-level and domain-level purification to an extent, i.e., we expect HA-LoRA to focus only on encoding rich *task-related* properties, while leaving the goal of selecting domain-invariant properties to domain-level purification. During training, we jointly train the head-aware LoRA and the gates of attention heads to perform the task

and domain-level purification simultaneously. Pre-trained parameters in the image encoder and the text encoder of CLIP are frozen throughout the training. We conduct extensive experiments on various representative domain generalization benchmarks including Office-Home (Venkateswara et al., 2017), DomainNet (Peng et al., 2019), PACS (Li et al., 2017), VLCS (Torralba & Efros, 2011) and TerraIncognita (Beery et al., 2018). All those experiments verify the superiority of our proposed method.

In a nutshell, our contributions can be summarized as **1)** We observe that not all attention heads of CLIP are domain generalizable in terms of specific tasks and propose a new perspective to harness CLIP for DG through attention head purification, *i.e.*, optimizing attention heads to make them more task-adapted and domain generalizable. **2)** We decouple the attention head purification from two levels including task-level purification and domain-level purification. We design head-aware LoRA and learnable gating strategy to perform the two kinds of purification respectively. **3)** Extensive experiments on representative domain generalization benchmarks demonstrate that our method performs favourably against the previous state-of-the-art.

2 RELATED WORKS

Vision-Language Pre-training. Vision-Language models (VLMs) connect images and texts through a common embedding space to enable cross-modal learning (Frome et al., 2013; Socher et al., 2013; Elhoseiny et al., 2013). Recent advances employ architectures with better representation learning abilities such as Transformer (Vaswani et al., 2017) and webscale training datasets and build stronger vision-language pre-trained models. One type of approach learns the common embedding space by masked language modeling or masked region prediction (Tan & Bansal, 2019; Su et al., 2019; Kim et al., 2021). Another typical type of vision-language pretraining is contrastive image-language pre-training, such as CLIP (Radford et al., 2021) and ALIGN (Jia et al., 2021). Recent research also seeks to improve the pre-training paradigm, such as using additional supervision (Li et al., 2021; Mu et al., 2022), employing pre-trained image encoders (Zhai et al., 2022), and adding cross-modal and in-modal consistency constraints (Goel et al., 2022). In this paper, instead of designing better pretraining techniques, we aim at utilizing recent advances in vision-language pre-trained models such as CLIP and achieving better generalization performance.

Domain Generalization (DG). Domain generalization aims to learn generalized representations from multiple source domains that can generalize well on arbitrary unseen target domains. Most DG methods perform domain alignment (Ganin & Lempitsky, 2015; Jia et al., 2020; Li et al., 2018c; Shao et al., 2019; Li et al., 2020; Wang et al., 2021; Ouyang & Key, 2021), to learn domain invariant features by reducing the distance of distributions across multiple domains. Specifically, to achieve domain-invariance, Jia et al. (2020); Li et al. (2018c); Shao et al. (2019); Ouyang & Key (2021); Ganin & Lempitsky (2015) imply adversarial learning, Ouyang & Key (2021) minimizes maximum mean discrepancy (MMD), and Sankaranarayanan & Balaji (2023); Balaji et al. (2018a); Dou et al. (2019) utilize meta-learning techniques. In addition, Zhou et al. (2020b); Cubuk et al. (2020); Li et al. (2022); Kang et al. (2022); Zhou et al. (2021); Nuriel et al. (2021); Li et al. (2023); Guo et al. (2023) use domain augmentation to enrich the style diversity of source data at image level or feature level. The remarkable progress achieved by those works can be largely attributed to a well-initialized feature extractor provided by ImageNet pre-training (Huh et al., 2016). Recent proposed Vision-language pre-trained models such as CLIP exhibit impressive zero-shot generalization ability. Its zero-shot performance exceeds the aforementioned methods in various DG tasks. In this paper, we focus on leveraging CLIP to further improve domain generalization performance.

CLIP-based Domain Generalization. Despite the good zero-shot performance, research finds that directly finetuning CLIP models with task-specific data will damage the alignment in joint vision-language spaces (Zhang et al., 2023b) and harm CLIP’s domain generalization ability (Radford et al., 2021; Wortsman et al., 2022). Recent advances explore adapting CLIP to downstream tasks without affecting its generalization ability by adapter learning (Gao et al., 2024; Zhang et al., 2021), model ensemble (Wortsman et al., 2022), regularized fine-tuning (Wortsman et al., 2022; Cha et al., 2022; Shu et al., 2023; Lew et al., 2023), distillation (Hémadou et al., 2023; Huang et al., 2023), and prompt learning (Cho et al., 2023; Zhou et al., 2022b; Zhang et al., 2023a; Niu et al., 2022; Bose et al., 2024; Cheng et al., 2024; Bai et al., 2024). Different from most existing works that use regularization to avoid knowledge forgetting of CLIP, we propose attention head purification to harness CLIP for DG.

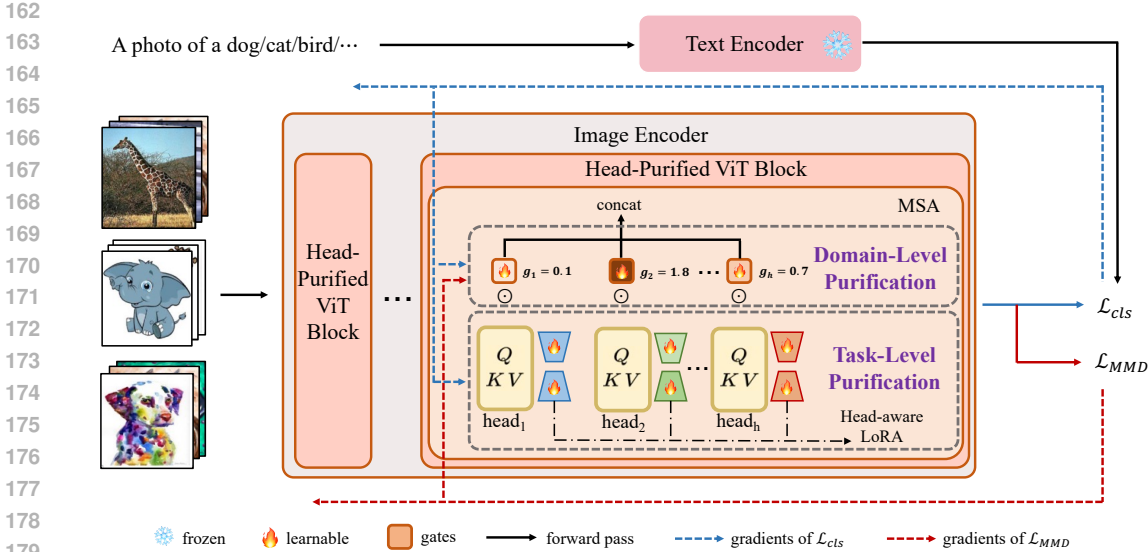


Figure 2: The architecture of Attention Head Purification. We design head-aware LoRA to perform task-level purification and domain-invariant gating strategy to perform domain-level purification. Further, we minimize \mathcal{L}_{cls} (Section 3.2.1) to update head-aware LoRA and minimize $\mathcal{L}_{cls}, \mathcal{L}_{MMD}$ (Section 3.2.2) to update the gates of heads.

3 METHOD

3.1 PRELIMINARY

Background. We aim to tackle the domain generalization problem based on CLIP. Specifically, suppose we have multiple source domains for training. Our goal is to adapt CLIP with labeled samples from source domains to make it perform well on unseen target domains. Usually, the distribution of target domain data is distinct from that of each source domain.

CLIP Revisiting. CLIP is a large-scale visual-language model that consists of an image encoder and a text encoder. CLIP is trained with 400 million web-scraped image-text pairs (Radford et al., 2021). The contrastive loss is imposed to encourage the features from paired image-text to be more aligned than unpaired ones. As a result, CLIP is readily adopted to downstream tasks even without any fine-tuning, showing impressive zero-shot classification ability. Specifically, given C classes with their class names, we may construct a text description for each class, e.g., “A photo of a #classname”. For a specific image, we extract its image feature, and compare the extracted image feature with text features of different classes. Then, the class of text feature which has a highest cosine similarity with the image feature is viewed as the predicted label of the image. Formally, the zero-shot classification process can be represented as $\hat{y} = \operatorname{argmax}_c \cos(I, T_c)$, where I denote the image feature, T_c denotes the text feature of class $c \in \{0, 1, 2, \dots, C - 1\}$, and \hat{y} is the predicted label for the image.

LoRA Revisiting. Low-rank adaptation (LoRA) (Hu et al., 2021) is one of the most popular parameter-efficient fine-tuning (PEFT) methods. It assumes that the changes of parameters lie in a low-rank space when the model is fine-tuned on a downstream task. Specifically, for a linear layer with the input dimension d_I and the output dimension d_O , we represent its weight with $W^{d_O \times d_I}$. Then LoRA reparametrizes the pre-trained weight W by expanding a branch with two matrices, $A \in R^{d_O \times r}$ and $B \in R^{r \times d_I}$. Typically, r is much smaller than the input dimension d_I and output dimension d_O , making A a dimension increasing matrix and B a dimension reduction matrix. Finally, LoRA modifies the forward propagation in this linear layer as $o = We + ABe$ where e and o denote the input and output features of this layer respectively. During adaptation to the downstream tasks, we freeze the pre-trained weight W and only update A and B .

3.2 ATTENTION HEAD PURIFICATION OF CLIP

Overall Framework. The image encoder of CLIP encodes rich properties of an image into image features. For a specific downstream task, not all properties are beneficial, *i.e.*, some properties may

not be task-related, and some properties may not be domain-invariant. As shown in Gandelsman et al. (2023), different attention heads may encode different properties of an image. From this point of view, we propose to purify the attention heads of CLIP from two levels, including task-level purification (detailed in Section 3.2.1) and domain-level purification (detailed in Section 3.2.2). For task-level purification, we purify the attention head of CLIP using our designed head-aware LoRA (HA-LoRA) to focus on task-related properties. For domain-level purification, we design a simple learnable gating strategy to emphasize generalizable heads while restraining domain-sensitive heads. During training, we add HA-LoRA and head gating into certain layers of CLIP’s image encoder as shown in Figure 2 to conduct task-level purification and domain-level purification simultaneously.

3.2.1 TASK-LEVEL PURIFICATION WITH HEAD-AWARE LORA

From the task-level, we use LoRA to purify each attention head, *i.e.*, encouraging the heads to focus on task-related patterns while ignoring task-irrelevant ones. Technically, for a linear projection W , we may add a branch which sequentially multiplies a dimension reduction matrix $B \in \mathbb{R}^{r \times d_I}$ and a dimension increasing matrix $A \in \mathbb{R}^{d_O \times r}$. Then, the forward propagation of this linear layer is modified as

$$o = We + AB e = W' e, \quad (1)$$

where $W' = W + AB$ denotes the adapted weight, e denotes the input of the projection, and o denotes the output. We only use LoRA to adapt the linear projections of query (Q) and value (V) in multi-head self-attention (MSA) blocks. To improve the effect of task-level purification and facilitate the following domain-level purification, we propose using head-aware LoRA instead of the conventional LoRA in our framework.

Head-aware LoRA. For the pre-trained weight $W \in \mathbb{R}^{d_O \times d_I}$ of the Q or V projection in a MSA block, we can split d_O into H groups (*i.e.*, W_1, W_2, \dots, W_H) where H denotes the number of attention heads in a MSA block. As a result, $W_h \in \mathbb{R}^{n \times d_I}$, $h \in \{1, 2, \dots, H\}$ where $n = d_O/H$. We split the matrix A in the same way and obtain A_1, A_2, \dots, A_H where $A_h \in \mathbb{R}^{n \times r}$. Then the adapted weight W' of the conventional LoRA can be reformulated as

$$W' = W + AB = W + \begin{pmatrix} A_1 B \\ A_2 B \\ \vdots \\ A_H B \end{pmatrix} = \begin{pmatrix} W_1 + A_1 B \\ W_2 + A_2 B \\ \vdots \\ W_H + A_H B \end{pmatrix}. \quad (2)$$

From Eq. (2), we observe that in the conventional LoRA, different from A_h which is distinct with respect to different heads, B is shared by all the heads. As a result, purifying one head may interfere with the other head, rendering the head purification less effective.

To mitigate such interference between different heads, we propose head-aware LoRA, denoted as HA-LoRA. As shown in Task-Level Purification module in Figure 2, we set independent $B_h \in \mathbb{R}^{r \times d_I}$ for each head. The adapted weight W' for HA-LoRA can be represented as:

$$W' = W + \begin{pmatrix} A_1 B_1 \\ A_2 B_2 \\ \vdots \\ A_H B_H \end{pmatrix} = \begin{pmatrix} W_1 + A_1 B_1 \\ W_2 + A_2 B_2 \\ \vdots \\ W_H + A_H B_H \end{pmatrix} \quad (3)$$

Different from Tian et al. (2024), which also uses independent B to handle different tasks, we use independent B to modulate different heads. The two approaches are technically similar but differ in their underlying motivations.

We follow the vision-language contrastive learning strategy to update the parameters of HA-LoRA. For each class c , we manually generate a text describing it, *e.g.*, “A photo of a #classname”. We then get the text embedding of each class T_c extracted by the text encoder. Then, we impose a contrastive loss between image features and the text features of different classes to encourage the image feature to be more aligned with the text feature of ground-truth label, *i.e.*,

$$\mathcal{L}_{cls} = -\frac{1}{N} \sum_{i=1}^N \log \frac{\exp(\cos(s_i, T_y)/\tau)}{\sum_{c=1}^C \exp(\cos(s_i, T_c)/\tau)} \quad (4)$$

where s_i denotes the image feature for the i -th sample, T_c denotes the text feature of class c , y is the ground-truth label for the i -th image and τ is the temperature hyper-parameter.

3.2.2 DOMAIN-LEVEL PURIFICATION WITH DOMAIN-INVARIANT GATING

By task-level purification, we can wipe off task-unrelated properties, making each head more adapted to current task. After this, we also need to perform domain-level purification, aiming to maintain or emphasize the most generalizable or invariant attention heads across domains. To realize this, we design a domain-invariant gating (DIG) scheme. Specifically, in a MSA block, we set a series of learnable gates g_1, g_2, \dots, g_H , the number of which equals the number of attention heads H . To evaluate the relative importance of each head, we apply softmax operation to the gates, *i.e.*, $\hat{g}_1, \hat{g}_2, \dots, \hat{g}_H = \text{Softmax}(g_1, g_2, \dots, g_H)$. Then, we apply the gates to the features of different heads which are the outputs of the scaled dot-product attention operation. We concatenate the gated features from all the heads and obtain f^g as

$$f^g = \gamma[\hat{g}_1 f_1, \hat{g}_2 f_2, \dots, \hat{g}_H f_H] \quad (5)$$

where f_1, f_2, \dots, f_H denote the features of different attention heads. The γ equals to the number of heads, which is used to compensate the scale changes after softmax operation.

During training, in addition to \mathcal{L}_{cls} , we also utilize Maximum Mean Discrepancy (MMD) loss (Long et al., 2015; 2017) to measure the distribution discrepancy of features between different source domains, *i.e.*,

$$\begin{aligned} \text{MMD}(S^p, S^q) &= \frac{1}{N^2} \sum_{i=1}^N \sum_{i'=1}^N k(s_i^p, s_{i'}^p) + \frac{1}{M^2} \sum_{j=1}^M \sum_{j'=1}^M k(s_j^q, s_{j'}^q) - \frac{2}{MN} \sum_{i=1}^N \sum_{j=1}^M k(s_i^p, s_j^q) \\ \mathcal{L}_{\text{MMD}} &= \frac{2}{d(d-1)} \sum_{p=1}^{d-1} \sum_{q=p+1}^d \text{MMD}(S^p, S^q) \end{aligned} \quad (6)$$

where $S^p = \{s_i^p\}_{i=1}^N$ are image features of p -th source domain output by CLIP’s image encoder, N denotes the number of samples for domain p within a mini-batch, d denotes the number of source domains and k denotes the Gaussian kernel (Long et al., 2015; 2017).

In this way, if the gates select/emphasize heads which are more generalizable, the resulting features are more generalizable, rendering \mathcal{L}_{MMD} small, otherwise the \mathcal{L}_{MMD} will be large. Thus, minimizing \mathcal{L}_{MMD} will encourage the gates to update towards selecting/emphasizing the most generalizable or domain-invariant heads.

3.3 OBJECTIVE

Since both task-level purification and domain-level purification contribute to CLIP’s domain generalization performance, we want to combine them to achieve further performance improvement. We perform end-to-end training that simultaneously conducts task-level purification and domain-level purification as shown in Figure 2. The final optimization objective is as follows

$$\min_{\theta_1, \theta_2} \alpha \mathcal{L}_{cls} + \min_{\theta_2} \alpha \mathcal{L}_{\text{MMD}}, \quad (7)$$

where $\theta_1 = \{A_1, A_2, \dots, A_H, B_1, B_2, \dots, B_H\}$, and $\theta_2 = \{g_1, g_2, \dots, g_H\}$. The α controls the strength of MMD loss.

As shown in Eq. (7), we do not use MMD loss to update HA-LoRA. In this way, we may decouple task-level and domain-level purification to an extent, *i.e.*, we expect HA-LoRA to focus only on encoding rich *task-related* properties, while leaving the goal of selecting domain-invariant properties to domain-level purification. For inference, we can merge HA-LoRA with the original weights of CLIP, eliminating extra memory overhead.

Head-aware LoRA vs. LoRA. Note that when jointly performing task-level and domain-level purification, head-aware LoRA is more beneficial to the domain-level purification than the convention LoRA. It is because different to conventional LoRA, head-aware LoRA owns different learnable parameters across different heads, which avoids the interference between different heads. Through such a head-interference elimination, the DIG may more independently and accordingly emphasize or restrain specific heads (see Section 5.1 for empirical details).

3.4 COMBINE WITH PROMPT-LEARNING METHODS

For classification with CLIP, we follow the general practice that comparing the similarity scores between the image feature and text features of difference classes. To generate the text feature of a

specific class, we need to conduct a text description which contains a prompt and the name of a class, and forward it through the text encoder of CLIP. The quality of prompt also affects the generalization ability of CLIP. Thus, many previous works, *e.g.*, CoOp (Zhou et al., 2022b), CoCoOp (Zhou et al., 2022a) and DPL (Zhang et al., 2023a) try to optimize the prompt to improve the generalization ability of CLIP. In this paper, we focus on how to extract more generalizable image features from CLIP, which is orthogonal to the previous prompt-learning methods. Thus, in practice, we may combine our method with previous prompt-learning method to maximize the generalization ability of CLIP across different domains, *i.e.*, we may utilize previous prompt-learning methods to optimize the prompt and employ our attention head purification to optimize the image features.

4 DATASETS AND IMPLEMENTATION DETAILS

4.1 DATASETS

For comparison, we evaluate our method on five representative datasets, including OfficeHome (Venkateswara et al., 2017), PACS (Li et al., 2017), VLCS (Torralla & Efros, 2011), TerraIncognita (Beery et al., 2018) and DomainNet (Peng et al., 2019). **OfficeHome** (OH) includes 4 domains with 15,588 examples from 65 classes. **VLCS** includes 4 domains with 10,729 examples from 5 classes. **PACS** includes 4 domains with 9,991 examples from 7 classes. **DomainNet** (DN) includes 6 domains with 586,575 examples from 345 classes. **TerraIncognita** (TI) includes 4 domains with 24788 examples from 10 classes. Following Xu et al. (2021); Ganin & Lempitsky (2015), we adopt the typical leave-one-domain-out protocol for evaluation, *i.e.*, each time we select one out of available domains as the target for testing and the remaining domains as sources for training. The average accuracy across all target choices is reported.

4.2 IMPLEMENTATION DETAILS

We use the CLIP pre-trained model with ViT-B/16 as the image encoder. We only tune the image encoder. The text encoder of CLIP is kept frozen throughout the training. The batch size is set to 36. We use the AdamW as the optimizer with the cosine learning rate strategy for all datasets. We use a learning rate of 5×10^{-5} for updating head-aware LoRA and 1×10^{-3} for optimizing the head gates. For each run, we train the model for 40 epochs. We report the average result over three runs with different random seeds. We set the temperature τ to 0.01 which is the same as the pre-trained model. The α is set to 0.2 and kept the same across all the datasets. We purify the attention heads in all layers of the image encoder, and impose the MMD loss on each layer. For all the experiments, the rank of our head-aware LoRA is set to 8 for the last two layers and 2 for the rest layers.

5 EXPERIMENTAL RESULTS

We evaluate the proposed method for domain generalization classification task. We first conduct an extensive ablation study to validate key components of our framework. Second, we show that the proposed method can be combined with prompt-learning techniques and obtain significant performance gain. This demonstrates that our attention head purification technique is complementary to a wide range of prompt-learning strategies and provides additional benefits. Third, we show that our model performs favorably against previous state-of-the-art approaches. Finally, we visualize the attention maps of the overall model and specific heads.

5.1 ABLATION STUDY

Task-level purification and domain-level purification cooperates to improve the generalization ability of CLIP. In Table 1 (Left), we verify the effectiveness of task-level purification with head-aware LoRA (“HA-LoRA”) and domain-level purification with domain-invariant gating (“DIG”). We observe that both task-level purification and domain-level purification contribute to the performance improvement compared to the zero-shot baseline (the first line in Table 1 (Left)). When combining both of them, we may further improve the domain generalization performance, obtaining 4.6% gain on OfficeHome and 3.4% gain on DomainNet compared to the zero-shot baseline. All those results verify the effectiveness of our proposed task-level purification and domain-level purification operations.

Head-aware LoRA eliminates interference between different heads, benefiting subsequent head selection in domain-level purification. In Table 1 (Right), we investigate the effect of our proposed HA-LoRA compared with the conventional LoRA. We find that without performing domain-level purification (*i.e.*, without using DIG), the result of HA-LoRA is only slightly better than that of the

Table 1: **Left:** Effect of task/domain-level purification. **Right:** Head-aware LoRA vs. original LoRA.

HA-LoRA	DIG	OfficeHome	DomainNet	LoRA	HA-LoRA	DIG	OfficeHome	DomainNet
		82.4	57.7	✓		w/o.	84.8	58.7
✓		85.0	58.8		✓	w/o.	85.0(+0.2%)	58.8(+0.1%)
	✓	83.6	58.2	✓		w.	86.0	59.7
✓	✓	87.0	61.1		✓	w.	87.0(+1.0%)	61.1(+1.4%)

conventional LoRA (around 0.1% gain). However, when jointly optimizing domain-invariant gates and LoRA/HA-loRA, HA-LoRA achieves a remarkable improvement compared to the conventional LoRA (more than 1% gain). This is because the proposed head-aware LoRA can effectively eliminate the interference between different heads. Through interference elimination, the DIG may more independently and accordingly emphasize or restrain specific heads, rendering the domain-level purification more effective.

Decoupling task-level purification and domain-level purification is beneficial. As discussed in Section 3.2.2, we adopt MMD loss to encourage the head gates in DIG to update towards making the features invariant across domains. Technically, we may also adopt MMD loss to update HA-LoRA to encourage HA-LoRA to encode both task-related and domain-invariant properties. But we find this will harm the generalization performance. In Table 2, we compare the training without imposing any MMD loss (the first line), using MMD loss to update HA-LoRA (the second line), using MMD loss to update both the head gates and HA-LoRA (the third line) and our solution that uses MMD loss to update the head gates only (the last line). We observe that our solution obviously outperforms the one without any MMD loss, showing that MMD loss contributes to selecting/emphasizing the most domain-generalizable attention heads. When applying MMD loss to update HA-LoRA, the performance decreases. It is because applying MMD to HA-LoRA may encourage HA-LoRA to be both task-adapted and domain-invariant. Such a coupled optimization is more difficult.

Joint purification training is the first choice. In Table 3 (Left), we investigate the effect of different training strategies, including ours which jointly trains HA-LoRA and DIG, alternatively training DIG and HA-LoRA (denoted as alternative), training DIG first and then training HA-LoRA with fixed DIG (domain→task), and training HA-LoRA first and then training DIG with fixed HA-LoRA (task→domain). We observe that ours achieves the best results among different training strategies.

Table 2: Performance of using \mathcal{L}_{MMD} to update different modules. Results show that we may not obtain domain generalizable features directly through encouraging domain-invariant HA-LoRA.

Modules that updated by \mathcal{L}_{MMD}	OfficeHome	DomainNet	PACS
Neither	86.2	60.5	96.9
HA-LoRA	85.8	58.6	96.1
HA-LoRA + DIG	86.0	59.9	96.7
DIG	87.0	61.1	98.1

Table 3: **Left:** Effect of different training strategies. **Right:** Sensitivity to the ratio α of MMD loss term. The experiments are conducted on OfficeHome. The trends are similar for the other datasets.

Method	OfficeHome	Values of α	OfficeHome
jointly	87.0	0.0	86.2
alternative	86.7	0.1	86.7
two-stage(Task → Domain)	85.8	0.2	87.0
two-stage(Domain → Task)	85.1	0.3	86.9
		0.5	86.7

Sensitivity to the ratio α of MMD loss term. In Table 3 (Right), we evaluate how the performance changes as α increases. We observe as α increases, the accuracy firstly increases and then decreases, exhibiting a typical bell curve. This phenomenon shows the regularization effect of MMD loss term. Besides, within a vast range of α , the accuracy only slightly fluctuates. Note that the trends are similar across all the datasets. The results show that our method is relatively robust to the choices of α .

5.2 IMPROVEMENT BEYOND PROMPT-LEARNING METHODS

In Table 4, we combine our method with representative prompt-learning DG methods. Besides, we also report numbers obtained by our method with manually designed prompt “A photo of a”

(same as zero-shot CLIP baseline). We observe that even without any prompt optimization, our method achieves remarkable improvement compared to zero-shot CLIP baseline (around 8% gain). Previous prompt-learning DG methods can be roughly categorized into two groups. One group, *e.g.*, DUPRG and PromptStyler, only utilizes text features to optimize the prompt. The other group, *e.g.*, CoOp, CoCoOp, DPL and STYLIP, utilizes the alignment between image features and text features to optimize the learnable prompt. Thus, for different groups, we combine attention head purification with prompt-learning in different ways. For the first group, we sequentially perform prompt optimization and attention head purification, *i.e.*, we firstly obtain optimized prompt with prompt-learning method and then utilize the optimized prompt in attention head purification learning. For the second group, we jointly learn attention head purification and optimize the prompt. As shown in Table 4, combining with attention head purification can consistently improve the generalization performance of CLIP beyond the prompt-learning methods, *e.g.*, combining attention head purification with PromptStyler yields the best result (79.0% average accuracy) with 5.5% improvement beyond PromptStyler.

Table 4: Improvement beyond prompt-learning methods. [†] indicates that the number is reproduced by us since the number is not provided in the original paper. Others are cited from the original paper.

Method	OH	VLCS	PACS	DN	TI	Avg.
Zero-Shot	82.4	81.7	96.1	56.6	33.8	70.1
+ours	87.0	85.1	98.1	61.1	59.7	78.2 (+8.1%)
CoOp [†] (Zhou et al., 2022b)	83.0	80.8	96.4	59.5	46.8	73.6
+ours	87.3	85.3	98.2	61.0	59.9	78.3 (+4.7%)
CoCoOp [†] (Zhou et al., 2022a)	83.4	80.3	96.7	59.4	45.3	73.2
+ours	87.4	84.8	98.4	61.3	58.8	78.2 (+5.0%)
DPL (Zhang et al., 2023a)	84.2	84.3	97.3	56.7	52.6 [†]	75.0
+ours	87.2	85.1	98.0	61.4	60.6	78.5 (+3.5%)
DUPRG (Niu et al., 2022)	83.6	83.9	97.1	59.6	42.0	73.2
+ours	87.0	85.4	98.2	61.5	60.1	78.4(+5.2%)
STYLIP [†] (Bose et al., 2024)	84.1	84.8	96.8	59.9	57.4	76.6
+ours	87.5	85.3	98.5	62.1	59.9	78.7(+2.1%)
PromptStyler (Cho et al., 2023)	83.6	82.9	97.2	59.4	44.2 [†]	73.5
+ours	87.7	86.1	98.3	62.0	60.6	79.0(+5.5%)

5.3 COMPARISON WITH PREVIOUS STATE-OF-THE-ARTS

In Table 5, we compare our solution with previous state-of-the-art CLIP-based domain generalization methods. Besides, we also compare our method to baselines including zero-shot CLIP (“zero-shot”), linear probing of CLIP (“Linear-Probe”), and standard full fine-tuning of CLIP with all source domains (“ERM-FFT”). We report the accuracy for each dataset and the average accuracy across all the datasets in Table 5 for comparison. [†] indicates that the number is reproduced by us since it is not provided in the original paper. Other numbers are cited from the original paper. For our method, we report numbers obtained by attention head purification combined with prompt learning (“Ours”).

From Table 5, we find that CLIP’s zero-shot result serves as a strong baseline. Directly linear probing or full fine-tuning CLIP’s image encoder even results in worse accuracy, demonstrating that it is non-trivial to harness CLIP for domain generalization tasks. For methods that fine-tune the image encoder, existing competitors, including GESTUR, MIRO, and CLIPood, mainly focus on avoiding knowledge forgetting of CLIP during task adaptation. Our method outperforms these methods, *e.g.*, outperforming MIRO by more than 5%, indicating that our way of performing attention head purification is more effective on improving the CLIP’s domain generalization performance. Overall, compared with various CLIP-based generalization methods, our method achieves the best result.

5.4 VISUALIZATION

We visualize the overall attention maps (Chefer et al., 2021) before and after attention head purification in Figure 3(a). We observe that the zero-shot model owns a sparser attention and pays more attention to the background which may not be generalizable across domains. In contrast, ours attends to the most discriminative and generalizable properties of the object for classification. We further visualize the attention maps generated by specific attention heads. We show the attention maps of the top two heads (Figure 3(b)(c)) and the last head (Figure 3(d)) ranked by the learned head gates. The top two

Table 5: Comparison with previous state-of-the-arts. † indicates that the number is reproduced by us as it is not reported by the original paper. Others are cited from the original paper.

Method	OH	VLCS	PACS	DN	TI	Avg.
Zero-Shot	82.4	81.7	96.1	56.6	33.8	70.1
Linear-Probe†	79.3	77.5	94.9	48.2	44.6	68.9
ERM-FFT†	80.0	79.1	91.4	53.9	44.1	69.7
CoOp† (Zhou et al., 2022b)	83.0	80.8	96.4	59.5	46.8	73.6
CoCoOp† (Zhou et al., 2022a)	83.4	80.3	96.7	59.4	45.3	73.2
MaPLe† (Khattak et al., 2023)	83.4	82.2	96.5	59.5	50.2	74.4
VPT† (Jia et al., 2022)	83.2	82.0	96.9	58.5	46.7	73.6
DPL (Zhang et al., 2023a)	84.2	84.3	97.3	56.7	52.6†	75.0
DUPRG (Niu et al., 2022)	83.6	83.9	97.1	59.6	42.0	73.2
PromptStyler (Cho et al., 2023)	83.6	82.9	97.2	59.4	44.2†	73.5
STYLIP (Bose et al., 2024)	84.6	86.9	98.1	62.0	57.4†	77.8
DSPL (Cheng et al., 2024)	86.1	86.4	97.5	62.1	57.1	77.8
SPG (Bai et al., 2024)	83.6	82.4	97.0	60.1	50.2	74.7
VL2V-SD (Addepalli et al., 2024)	85.4	82.7	95.7	58.7	41.2	72.7
CLIP-LoRA† (Zanella & Ben Ayed, 2024)	83.9	83.1	97.1	58.4	55.7	75.6
GESTUR (Lew et al., 2023)	84.2	82.8	96.0	58.9	55.7	75.5
MIRO (Cha et al., 2022)	82.5	82.2	95.6	54.0	54.3	73.7
CLIPood (Shu et al., 2023)	87.0	85.0	97.3	63.5	60.4	78.6
CLIPood† (Shu et al., 2023)	85.3	83.6	97.3	59.5	58.7	76.9
Ours	87.7±0.1	86.1±0.3	98.3±0.2	62.0±0.1	60.6±0.4	79.0

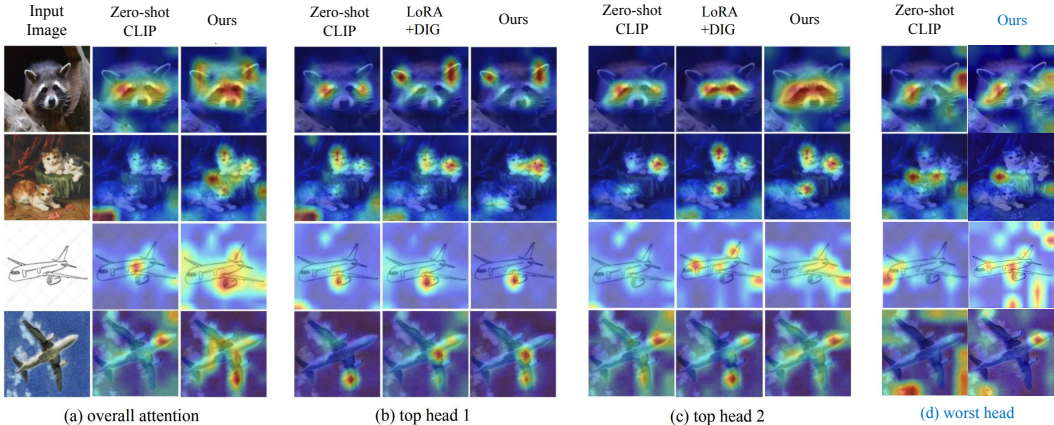


Figure 3: Attention maps for target samples in DomainNet.

heads exhibit different preferences. Generally, top head 1 tends to capture the most discriminative part of each object, for example, the ear of a raccoon (first row) and the engine of a plane (third row), while top head 2 tends to focus on the overall region of an object. Besides, compared with purifying heads using conventional LoRA with DIG (middle column in Figure 3 (b)(c)), thanks to the interference elimination of HA-LoRA, our method can better highlight the perceptual tendency of a specific head. For the worst head, as shown in Figure 3(d), background areas receive high attention. By assigning less weight to such heads in our method, their influence is suppressed.

6 CONCLUSION

In this paper, we propose a simple yet effective method to harness CLIP for domain generalization, *i.e.*, attention head purification. Specifically, we perform attention head purification from two perspectives including task-level purification and domain-level purification. For task-level purification, we design head-aware LoRA to make each head specifically adapted to the downstream tasks. For domain-level purification, we adopt a domain-invariant gating strategy to encourage the model to select/emphasize the most generalizable attention heads. During training, we jointly perform the task-level purification and the domain-level purification. Experiments on five representative domain generalization benchmarks demonstrate the superiority of our proposed method.

REFERENCES

- 540
541
542 Sravanti Addepalli, Ashish Ramayee Asokan, Lakshay Sharma, and R Venkatesh Babu. Leveraging
543 vision-language models for improving domain generalization in image classification. In *Proceed-*
544 *ings of the IEEE/CVF Conference on Computer Vision and Pattern Recognition*, pp. 23922–23932,
545 2024.
- 546 Shuanghao Bai, Yuedi Zhang, Wanqi Zhou, Zhirong Luan, and Badong Chen. Soft prompt generation
547 for domain generalization. *arXiv preprint arXiv:2404.19286*, 2024.
- 548
549 Yogesh Balaji, Swami Sankaranarayanan, and Rama Chellappa. Metareg: Towards domain gen-
550 eralization using meta-regularization. *Advances in neural information processing systems*, 31,
551 2018a.
- 552 Yogesh Balaji, Swami Sankaranarayanan, and Rama Chellappa. Metareg: Towards domain gen-
553 eralization using meta-regularization. *Advances in neural information processing systems*, 31,
554 2018b.
- 555
556 Sara Beery, Grant Van Horn, and Pietro Perona. Recognition in terra incognita. In *Proceedings of the*
557 *European conference on computer vision (ECCV)*, pp. 456–473, 2018.
- 558 Shirsha Bose, Ankit Jha, Enrico Fini, Mainak Singha, Elisa Ricci, and Biplab Banerjee. Stylib: Multi-
559 scale style-conditioned prompt learning for clip-based domain generalization. In *Proceedings of*
560 *the IEEE/CVF Winter Conference on Applications of Computer Vision*, pp. 5542–5552, 2024.
- 561
562 Fabio M Carlucci, Antonio D’Innocente, Silvia Bucci, Barbara Caputo, and Tatiana Tommasi.
563 Domain generalization by solving jigsaw puzzles. In *Proceedings of the IEEE/CVF Conference on*
564 *Computer Vision and Pattern Recognition*, pp. 2229–2238, 2019.
- 565 Junbum Cha, Kyungjae Lee, Sungrae Park, and Sanghyuk Chun. Domain generalization by mutual-
566 information regularization with pre-trained models. In *European conference on computer vision*,
567 pp. 440–457. Springer, 2022.
- 568
569 Hila Chefer, Shir Gur, and Lior Wolf. Generic attention-model explainability for interpreting bi-modal
570 and encoder-decoder transformers. In *Proceedings of the IEEE/CVF International Conference on*
571 *Computer Vision*, pp. 397–406, 2021.
- 572 De Cheng, Zhipeng Xu, Xinyang Jiang, Nannan Wang, Dongsheng Li, and Xinbo Gao. Disentangled
573 prompt representation for domain generalization. In *Proceedings of the IEEE/CVF Conference on*
574 *Computer Vision and Pattern Recognition*, pp. 23595–23604, 2024.
- 575
576 Junhyeong Cho, Gilhyun Nam, Sungyeon Kim, Hunmin Yang, and Suha Kwak. Promptstyler:
577 Prompt-driven style generation for source-free domain generalization. In *Proceedings of the*
578 *IEEE/CVF International Conference on Computer Vision*, pp. 15702–15712, 2023.
- 579 Ekin D Cubuk, Barret Zoph, Jonathon Shlens, and Quoc V Le. Randaugment: Practical automated
580 data augmentation with a reduced search space. In *Proceedings of the IEEE/CVF conference on*
581 *computer vision and pattern recognition workshops*, pp. 702–703, 2020.
- 582
583 Qi Dou, Daniel Coelho de Castro, Konstantinos Kamnitsas, and Ben Glocker. Domain generalization
584 via model-agnostic learning of semantic features. *Advances in neural information processing*
585 *systems*, 32, 2019.
- 586 Mohamed Elhoseiny, Babak Saleh, and Ahmed Elgammal. Write a classifier: Zero-shot learning using
587 purely textual descriptions. In *Proceedings of the IEEE International Conference on Computer*
588 *Vision*, pp. 2584–2591, 2013.
- 589
590 Andrea Frome, Greg S Corrado, Jon Shlens, Samy Bengio, Jeff Dean, Marc’Aurelio Ranzato,
591 and Tomas Mikolov. Devise: A deep visual-semantic embedding model. *Advances in neural*
592 *information processing systems*, 26, 2013.
- 593
Yossi Gandelsman, Alexei A Efros, and Jacob Steinhardt. Interpreting clip’s image representation via
text-based decomposition. *arXiv preprint arXiv:2310.05916*, 2023.

- 594 Yaroslav Ganin and Victor Lempitsky. Unsupervised domain adaptation by backpropagation. In
595 *International conference on machine learning*, pp. 1180–1189. PMLR, 2015.
- 596
- 597 Peng Gao, Shijie Geng, Renrui Zhang, Teli Ma, Rongyao Fang, Yongfeng Zhang, Hongsheng Li, and
598 Yu Qiao. Clip-adapter: Better vision-language models with feature adapters. *International Journal*
599 *of Computer Vision*, 132(2):581–595, 2024.
- 600
- 601 Shashank Goel, Hritik Bansal, Sumit Bhatia, Ryan Rossi, Vishwa Vinay, and Aditya Grover. Cyclip:
602 Cyclic contrastive language-image pretraining. *Advances in Neural Information Processing*
603 *Systems*, 35:6704–6719, 2022.
- 604
- 605 Ishaan Gulrajani and David Lopez-Paz. In search of lost domain generalization. *arXiv preprint*
606 *arXiv:2007.01434*, 2020.
- 607
- 608 Jintao Guo, Na Wang, Lei Qi, and Yinghuan Shi. Aloft: A lightweight mlp-like architecture with
609 dynamic low-frequency transform for domain generalization. In *Proceedings of the IEEE/CVF*
610 *Conference on Computer Vision and Pattern Recognition*, pp. 24132–24141, 2023.
- 611
- 612 Louis H emadou, H el ena Vorobieva, Ewa Kijak, and Frederic Jurie. Beyond internet images: Evaluat-
613 ing vision-language models for domain generalization on synthetic-to-real industrial datasets. In
614 *Synthetic Data for Computer Vision Workshop@ CVPR 2024*.
- 615
- 616 Edward J Hu, Yelong Shen, Phillip Wallis, Zeyuan Allen-Zhu, Yuanzhi Li, Shean Wang, Lu Wang,
617 and Weizhu Chen. Lora: Low-rank adaptation of large language models. *arXiv preprint*
618 *arXiv:2106.09685*, 2021.
- 619
- 620 Zeyi Huang, Andy Zhou, Zijian Ling, Mu Cai, Haohan Wang, and Yong Jae Lee. A sentence speaks
621 a thousand images: Domain generalization through distilling clip with language guidance. In
622 *Proceedings of the IEEE/CVF International Conference on Computer Vision*, pp. 11685–11695,
623 2023.
- 624
- 625 Minyoung Huh, Pulkit Agrawal, and Alexei A Efros. What makes imagenet good for transfer
626 learning? *arXiv preprint arXiv:1608.08614*, 2016.
- 627
- 628 Iris AM Huijben, Wouter Kool, Max B Paulus, and Ruud JG Van Sloun. A review of the gumbel-max
629 trick and its extensions for discrete stochasticity in machine learning. *IEEE Transactions on*
630 *Pattern Analysis and Machine Intelligence*, 45(2):1353–1371, 2022.
- 631
- 632 Chao Jia, Yinfei Yang, Ye Xia, Yi-Ting Chen, Zarana Parekh, Hieu Pham, Quoc Le, Yun-Hsuan Sung,
633 Zhen Li, and Tom Duerig. Scaling up visual and vision-language representation learning with
634 noisy text supervision. In *International conference on machine learning*, pp. 4904–4916. PMLR,
635 2021.
- 636
- 637 Menglin Jia, Luming Tang, Bor-Chun Chen, Claire Cardie, Serge Belongie, Bharath Hariharan, and
638 Ser-Nam Lim. Visual prompt tuning. In *European Conference on Computer Vision*, pp. 709–727.
639 Springer, 2022.
- 640
- 641 Yunpei Jia, Jie Zhang, Shiguang Shan, and Xilin Chen. Single-side domain generalization for face
642 anti-spoofing. In *Proceedings of the IEEE/CVF Conference on Computer Vision and Pattern*
643 *Recognition*, pp. 8484–8493, 2020.
- 644
- 645 Juwon Kang, Sohyun Lee, Namyup Kim, and Suha Kwak. Style neophile: Constantly seeking novel
646 styles for domain generalization. In *Proceedings of the IEEE/CVF Conference on Computer Vision*
647 *and Pattern Recognition*, pp. 7130–7140, 2022.
- 648
- 649 Muhammad Uzair Khattak, Hanoona Rasheed, Muhammad Maaz, Salman Khan, and Fahad Shahbaz
650 Khan. Maple: Multi-modal prompt learning. In *Proceedings of the IEEE/CVF Conference on*
651 *Computer Vision and Pattern Recognition*, pp. 19113–19122, 2023.
- 652
- 653 Donghyun Kim, Kaihong Wang, Stan Sclaroff, and Kate Saenko. A broad study of pre-training for
654 domain generalization and adaptation. In *European Conference on Computer Vision*, pp. 621–638.
655 Springer, 2022.

- 648 Wonjae Kim, Bokyung Son, and Ildoo Kim. Vilt: Vision-and-language transformer without convo-
649 lution or region supervision. In *International conference on machine learning*, pp. 5583–5594.
650 PMLR, 2021.
- 651 Byounggyu Lew, Donghyun Son, and Buru Chang. Gradient estimation for unseen domain risk
652 minimization with pre-trained models. In *Proceedings of the IEEE/CVF International Conference*
653 *on Computer Vision*, pp. 4436–4446, 2023.
- 654 Chenming Li, Daoan Zhang, Wenjian Huang, and Jianguo Zhang. Cross contrasting feature pertur-
655 bation for domain generalization. In *Proceedings of the IEEE/CVF International Conference on*
656 *Computer Vision*, pp. 1327–1337, 2023.
- 657 Da Li, Yongxin Yang, Yi-Zhe Song, and Timothy M Hospedales. Deeper, broader and artier domain
658 generalization. In *Proceedings of the IEEE international conference on computer vision*, pp.
659 5542–5550, 2017.
- 660 Da Li, Yongxin Yang, Yi-Zhe Song, and Timothy Hospedales. Learning to generalize: Meta-learning
661 for domain generalization. In *Proceedings of the AAAI conference on artificial intelligence*,
662 volume 32, 2018a.
- 663 Haoliang Li, Sinno Jialin Pan, Shiqi Wang, and Alex C Kot. Domain generalization with adversarial
664 feature learning. In *Proceedings of the IEEE conference on computer vision and pattern recognition*,
665 pp. 5400–5409, 2018b.
- 666 Haoliang Li, YuFei Wang, Renjie Wan, Shiqi Wang, Tie-Qiang Li, and Alex Kot. Domain generaliza-
667 tion for medical imaging classification with linear-dependency regularization. *Advances in neural*
668 *information processing systems*, 33:3118–3129, 2020.
- 669 Xiaotong Li, Yongxing Dai, Yixiao Ge, Jun Liu, Ying Shan, and Ling-Yu Duan. Uncertainty modeling
670 for out-of-distribution generalization. *arXiv preprint arXiv:2202.03958*, 2022.
- 671 Ya Li, Xinmei Tian, Mingming Gong, Yajing Liu, Tongliang Liu, Kun Zhang, and Dacheng Tao.
672 Deep domain generalization via conditional invariant adversarial networks. In *Proceedings of the*
673 *European conference on computer vision (ECCV)*, pp. 624–639, 2018c.
- 674 Yangguang Li, Feng Liang, Lichen Zhao, Yufeng Cui, Wanli Ouyang, Jing Shao, Fengwei Yu, and
675 Junjie Yan. Supervision exists everywhere: A data efficient contrastive language-image pre-training
676 paradigm. *arXiv preprint arXiv:2110.05208*, 2021.
- 677 Mingsheng Long, Yue Cao, Jianmin Wang, and Michael Jordan. Learning transferable features with
678 deep adaptation networks. In *International conference on machine learning*, pp. 97–105. PMLR,
679 2015.
- 680 Mingsheng Long, Han Zhu, Jianmin Wang, and Michael I Jordan. Deep transfer learning with joint
681 adaptation networks. In *International conference on machine learning*, pp. 2208–2217. PMLR,
682 2017.
- 683 Norman Mu, Alexander Kirillov, David Wagner, and Saining Xie. Slip: Self-supervision meets
684 language-image pre-training. In *European conference on computer vision*, pp. 529–544. Springer,
685 2022.
- 686 Hongjing Niu, Hanting Li, Feng Zhao, and Bin Li. Domain-unified prompt representations for
687 source-free domain generalization. *arXiv preprint arXiv:2209.14926*, 2022.
- 688 Oren Nuriel, Sagie Benaim, and Lior Wolf. Permuted adain: Reducing the bias towards global
689 statistics in image classification. In *Proceedings of the IEEE/CVF Conference on Computer Vision*
690 *and Pattern Recognition*, pp. 9482–9491, 2021.
- 691 Liwen Ouyang and Aaron Key. Maximum mean discrepancy for generalization in the presence of
692 distribution and missingness shift. *arXiv preprint arXiv:2111.10344*, 2021.
- 693 Xingchao Peng, Qinxun Bai, Xide Xia, Zijun Huang, Kate Saenko, and Bo Wang. Moment matching
694 for multi-source domain adaptation. In *Proceedings of the IEEE/CVF international conference on*
695 *computer vision*, pp. 1406–1415, 2019.

- 702 Hieu Pham, Zihang Dai, Golnaz Ghiasi, Kenji Kawaguchi, Hanxiao Liu, Adams Wei Yu, Jiahui Yu,
703 Yi-Ting Chen, Minh-Thang Luong, Yonghui Wu, et al. Combined scaling for zero-shot transfer
704 learning. *Neurocomputing*, 555:126658, 2023.
- 705
706 Fengchun Qiao, Long Zhao, and Xi Peng. Learning to learn single domain generalization. In
707 *Proceedings of the IEEE/CVF conference on computer vision and pattern recognition*, pp. 12556–
708 12565, 2020.
- 709 Alec Radford, Jong Wook Kim, Chris Hallacy, Aditya Ramesh, Gabriel Goh, Sandhini Agarwal,
710 Girish Sastry, Amanda Askell, Pamela Mishkin, Jack Clark, et al. Learning transferable visual
711 models from natural language supervision. In *International conference on machine learning*, pp.
712 8748–8763. PMLR, 2021.
- 713 Swami Sankaranarayanan and Yogesh Balaji. Meta learning for domain generalization. In *Meta*
714 *Learning With Medical Imaging and Health Informatics Applications*, pp. 75–86. Elsevier, 2023.
- 715
716 Rui Shao, Xiangyuan Lan, Jiawei Li, and Pong C Yuen. Multi-adversarial discriminative deep domain
717 generalization for face presentation attack detection. In *Proceedings of the IEEE/CVF conference*
718 *on computer vision and pattern recognition*, pp. 10023–10031, 2019.
- 719 Yang Shu, Xingzhuo Guo, Jialong Wu, Ximei Wang, Jianmin Wang, and Mingsheng Long. Clipood:
720 Generalizing clip to out-of-distributions. In *International Conference on Machine Learning*, pp.
721 31716–31731. PMLR, 2023.
- 722
723 Richard Socher, Milind Ganjoo, Christopher D Manning, and Andrew Ng. Zero-shot learning through
724 cross-modal transfer. *Advances in neural information processing systems*, 26, 2013.
- 725
726 Weijie Su, Xizhou Zhu, Yue Cao, Bin Li, Lewei Lu, Furu Wei, and Jifeng Dai. V1-bert: Pre-training
727 of generic visual-linguistic representations. *arXiv preprint arXiv:1908.08530*, 2019.
- 728 Hao Tan and Mohit Bansal. Lxmert: Learning cross-modality encoder representations from trans-
729 formers. *arXiv preprint arXiv:1908.07490*, 2019.
- 730
731 Chunlin Tian, Zhan Shi, Zhijiang Guo, Li Li, and Chengzhong Xu. Hydralora: An asymmetric lora
732 architecture for efficient fine-tuning. *arXiv preprint arXiv:2404.19245*, 2024.
- 733 Antonio Torralba and Alexei A Efros. Unbiased look at dataset bias. In *CVPR 2011*, pp. 1521–1528.
734 IEEE, 2011.
- 735
736 Ashish Vaswani, Noam Shazeer, Niki Parmar, Jakob Uszkoreit, Llion Jones, Aidan N Gomez, Łukasz
737 Kaiser, and Illia Polosukhin. Attention is all you need. *Advances in neural information processing*
738 *systems*, 30, 2017.
- 739 Hemanth Venkateswara, Jose Eusebio, Shayok Chakraborty, and Sethuraman Panchanathan. Deep
740 hashing network for unsupervised domain adaptation. In *Proceedings of the IEEE conference on*
741 *computer vision and pattern recognition*, pp. 5018–5027, 2017.
- 742
743 Riccardo Volpi, Hongseok Namkoong, Ozan Sener, John C Duchi, Vittorio Murino, and Silvio
744 Savarese. Generalizing to unseen domains via adversarial data augmentation. *Advances in neural*
745 *information processing systems*, 31, 2018.
- 746
747 Jindong Wang, Cuiling Lan, Chang Liu, Yidong Ouyang, Tao Qin, Wang Lu, Yiqiang Chen, Wenjun
748 Zeng, and S Yu Philip. Generalizing to unseen domains: A survey on domain generalization. *IEEE*
transactions on knowledge and data engineering, 35(8):8052–8072, 2022.
- 749
750 Ziqi Wang, Marco Loog, and Jan Van Gemert. Respecting domain relations: Hypothesis invariance
751 for domain generalization. In *2020 25th International Conference on Pattern Recognition (ICPR)*,
752 pp. 9756–9763. IEEE, 2021.
- 753
754 Mitchell Wortsman, Gabriel Ilharco, Jong Wook Kim, Mike Li, Simon Kornblith, Rebecca Roelofs,
755 Raphael Gontijo Lopes, Hannaneh Hajishirzi, Ali Farhadi, Hongseok Namkoong, et al. Robust
fine-tuning of zero-shot models. In *Proceedings of the IEEE/CVF conference on computer vision*
and pattern recognition, pp. 7959–7971, 2022.

- 756 Qinwei Xu, Ruipeng Zhang, Ya Zhang, Yanfeng Wang, and Qi Tian. A fourier-based framework
757 for domain generalization. In *Proceedings of the IEEE/CVF conference on computer vision and*
758 *pattern recognition*, pp. 14383–14392, 2021.
- 759 Maxime Zanella and Ismail Ben Ayed. Low-rank few-shot adaptation of vision-language models.
760 In *Proceedings of the IEEE/CVF Conference on Computer Vision and Pattern Recognition*, pp.
761 1593–1603, 2024.
- 762 Xiaohua Zhai, Xiao Wang, Basil Mustafa, Andreas Steiner, Daniel Keysers, Alexander Kolesnikov,
763 and Lucas Beyer. Lit: Zero-shot transfer with locked-image text tuning. In *Proceedings of the*
764 *IEEE/CVF Conference on Computer Vision and Pattern Recognition*, pp. 18123–18133, 2022.
- 765 Renrui Zhang, Rongyao Fang, Wei Zhang, Peng Gao, Kunchang Li, Jifeng Dai, Yu Qiao, and
766 Hongsheng Li. Tip-adapter: Training-free clip-adapter for better vision-language modeling. *arXiv*
767 *preprint arXiv:2111.03930*, 2021.
- 768 Xin Zhang, Shixiang Shane Gu, Yutaka Matsuo, and Yusuke Iwasawa. Domain prompt learning for
769 efficiently adapting clip to unseen domains. *Transactions of the Japanese Society for Artificial*
770 *Intelligence*, 38(6):B–MC2_1, 2023a.
- 771 Yuhui Zhang, Jeff Z HaoChen, Shih-Cheng Huang, Kuan-Chieh Wang, James Zou, and Serena Yeung.
772 Diagnosing and rectifying vision models using language. *arXiv preprint arXiv:2302.04269*, 2023b.
- 773 Kaiyang Zhou, Yongxin Yang, Timothy Hospedales, and Tao Xiang. Learning to generate novel
774 domains for domain generalization. In *Computer Vision–ECCV 2020: 16th European Conference,*
775 *Glasgow, UK, August 23–28, 2020, Proceedings, Part XVI 16*, pp. 561–578. Springer, 2020a.
- 776 Kaiyang Zhou, Yongxin Yang, Timothy Hospedales, and Tao Xiang. Deep domain-adversarial
777 image generation for domain generalisation. In *Proceedings of the AAAI conference on artificial*
778 *intelligence*, volume 34, pp. 13025–13032, 2020b.
- 779 Kaiyang Zhou, Yongxin Yang, Yu Qiao, and Tao Xiang. Domain generalization with mixstyle. *arXiv*
780 *preprint arXiv:2104.02008*, 2021.
- 781 Kaiyang Zhou, Jingkang Yang, Chen Change Loy, and Ziwei Liu. Conditional prompt learning for
782 vision-language models. In *Proceedings of the IEEE/CVF conference on computer vision and*
783 *pattern recognition*, pp. 16816–16825, 2022a.
- 784 Kaiyang Zhou, Jingkang Yang, Chen Change Loy, and Ziwei Liu. Learning to prompt for vision-
785 language models. *International Journal of Computer Vision*, 130(9):2337–2348, 2022b.

791 A APPENDIX

792 A.1 ATTENTION HEAD EVALUATION STRATEGY MENTIONED IN FIGURE 1

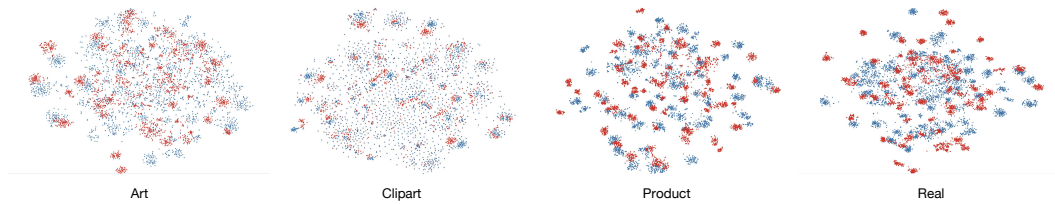
793 In Figure 1(a), we evaluate the importance of attention heads for domain generalization tasks with
794 different strategies including “randomly drop”, “manually drop”, “drop by cross-validation”, and
795 “adapt & drop”. We introduce the implementation details of each strategy as follows:

796 **Randomly drop:** we randomly sample a certain number of attention heads and drop them for
797 inference. We repeat the random sampling three times and report the average results.

800 **Manually drop:** we manually evaluate the generalization performance of each head based on the
801 text describing the properties of each head provided in Gandelsman et al. (2023) and then drop the
802 least generalizable heads for inference.

803 **Drop by cross-validation:** Each time we select one domain out of available domains as the target
804 domain for evaluation. We use the remaining domains to train the model to learn the importance of
805 each head for domain generalization task. Specifically, we adopt \mathcal{L}_{cls} to train a learnable Bernoulli
806 gate for each head representing the probability to remain the head, with the help of Gumbel-Softmax
807 trick (Huijben et al., 2022). During inference, we drop heads with probability from lowest to highest.
808 The CLIP is frozen during training. We report the average accuracy over different target domains.
809

810 **Adapt & drop**: following the above cross-validation setup, we perform attention head adaptation
 811 with LoRA and learn the gates simultaneously.
 812



813
 814
 815
 816
 817
 818
 819
 820
 821 Figure 4: t-SNE visualization of features from target domain on OfficeHome. We compare the
 822 visualization results of the original feature (blue dot) and our method (red dot).
 823

824
 825 Table 6: **Left**: Effect of soft gating in domain-level purification. **Right**: Training and inference time
 826 on DomainNet. Experiments were conducted on a single RTX4090 24Gb with the original code
 827 provided by the authors.
 828

Gating Strategy	PACS	OfficeHome	DomainNet	Method	Training time	Inference time
binary mask	96.9	85.4	57.7	CoOp	2h 57min.	39s
soft gating	98.1	87.0	61.1	DPL	2h	41s
				MIRO	5h 24min.	39s
				CLIPood	4h 46min.	39s
				Ours	1h 30min.	39s

833 834 835 A.2 PERFORMING DIG USING BINARY MASK INSTEAD OF SOFT GATING 836

837 With the help of Gumbel-Softmax trick, we can generate binary mask for attention heads to fully
 838 retain or remove a specific head. In Table 6 (Left), we provide the results of replacing soft gating
 839 with binary mask in DIG. We find that soft gating yields better performance.
 840

841 A.3 VISUALIZATION WITH T-SNE 842

843 We present the t-SNE visualization of the feature distribution on OfficeHome in Figure 4. The blue
 844 dots denote CLIP’s original visual feature and the red dots denote visual features generated by our
 845 method. For the original visual features, feature distribution is more dispersed especially for the
 846 domain Clipart. Nevertheless, benefiting from the attention head purification, the features of ours
 847 are more compact and the distribution is more concentrated, which is in line with the superior domain
 848 generalization performance of our method.
 849

850 A.4 COMPUTATIONAL EFFICIENCY

851 Table 6 (Right) compares the training time of the leading prompt-learning methods (CoOp (Zhou
 852 et al., 2022b) and DPL (Zhang et al., 2023a)) and fine-tuning methods (MIRO (Cha et al., 2022) and
 853 CLIPood (Shu et al., 2023)). Our method achieves better performance with shorter training time. We
 854 evaluate the inference time for each method on the “Real” domain of DomainNet dataset, with batch
 855 size set to 128. We observe that our method doesn’t introduce additional inference time compared to
 856 previous works.
 857

858 A.5 EFFECT OF FINE-TUNING THE TEXT ENCODER 859

860 The text features with specifically designed prompt in nature contain rare domain-specific information.
 861 Additionally, co-adapting the image encoder and text encoder on limited data can lead to overfitting,
 862 potentially disrupting the alignment between image and text features. As a result, we freeze the text
 863 encoder. As shown in Table 7, co-adapting the image and text encoders results in notable performance
 degradation.

Table 7: Effect of fine-tuning CLIP’s text encoder. We compare the results of co-adapting image encoder and text encoder with those of ours which freezes the text encoder.

Method	OH	PACS
Ours w. fine-tuning text encoder	84.7	96.5
Ours w.o. fine-tuning text encoder	87.0	98.1

A.6 VISUALIZATIONS WITH OVERALL ATTENTION

In Figure 5, we compare the overall attention maps of Head-Aware LoRA with DIG (our method), conventional LoRA with DIG, and the regularization-based method CLIPood. Our method generates better attention, enabling a more accurate and comprehensive perception of discriminative parts of the target object.

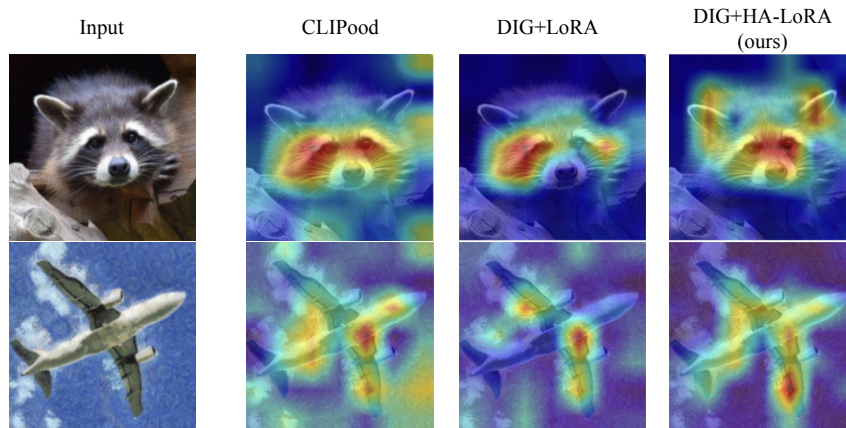


Figure 5: Comparison of the overall attention. Images are sampled from the DomainNet dataset. The “Real” is selected as the target domain while others are selected as source domains to train the CLIP.

A.7 VISUALIZATION WITH LEARNED GATING WEIGHTS OF DIG

In Figure 6, we visualize the learned gating weights of DIG. The observation is that the weight distribution is non-uniform, and there exists an apparent gap between the largest weight and the smallest weight. The results demonstrate that with DIG, some heads are relatively emphasized and some heads are relatively suppressed.

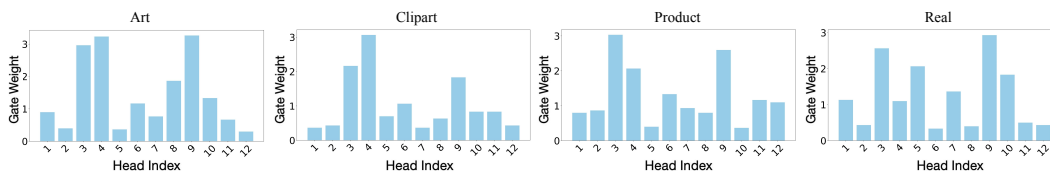
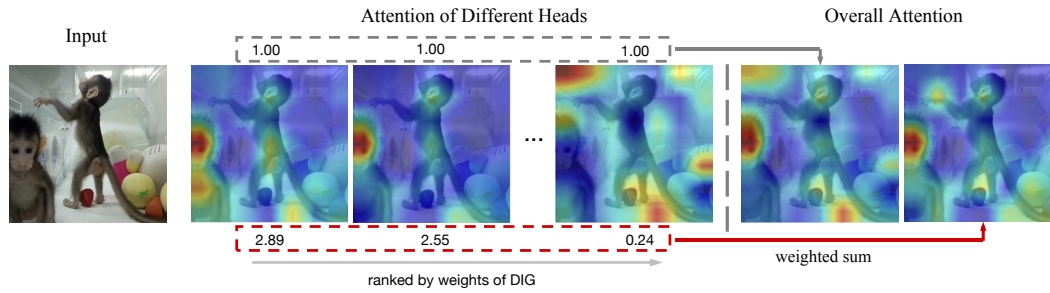


Figure 6: Distribution of the learned gating weights of DIG. Models are trained on OfficeHome. The domain name refers to the target domain in each case. The gate weights are not within 0-1 since we multiply the gates after Softmax operation \hat{g} by the number of heads γ , as shown in Equation (5).

A.8 EFFECTIVENESS OF DIG IN REMOVING DOMAIN-SPECIFIC INFORMATION.

In Figure 7, we provide attention to show the effectiveness of DIG in removing domain-specific information. The attention of different heads is ranked by the weights of DIG. For illustration purposes, we visualize the overall attention by aggregating the attention from all the heads. Purely

918 using HA-LoRA, the weights of different head attentions are equal to 1 for aggregating, while with
 919 DIG, the weights of different heads are different. From DIG ranking, we observe that the attention
 920 map which focuses on the discriminative parts of target object owns a larger gate weight while the
 921 attention map which focuses on the object-irrelevant background area owns a smaller gate weight.
 922 As a result, we observe that with the application of DIG, the domain-specific components (*e.g.*,
 923 background regions) in the overall attention are effectively suppressed, allowing better focus on the
 924 target object (*e.g.*, the monkey).



935 **Figure 7: Effectiveness of DIG in removing domain-specific information.** For illustration purpose,
 936 the overall attention is computed as a weighted sum of attention from different heads, using either
 937 DIG weights (as shown in red color) or uniform weights (*i.e.*, without DIG, as shown in gray color).
 938

939
940
941
942
943
944
945
946
947
948
949
950
951
952
953
954
955
956
957
958
959
960
961
962
963
964
965
966
967
968
969
970
971